# Contactless measurement of muscle fiber conduction velocity—a novel approach using optically pumped magnetometers

Journal of Neural Engineering

PAPER

# Contactless measurement of muscle fiber conduction velocity—a novel approach using optically pumped magnetometers

Lukas Baier[1,2,3,4], Tim Brümmer[1,2,3,4], Burak Senay[1,2,3,4], Markus Siegel[1,2,3], Ahmet Doğukan Keleş[4], Oliver Röhrle[4,5], Thomas Klotz[4], Nima Noury[1,2,3] and Justus Marquetand[1,2,3,4,*]

[1] Department of Neural Dynamics and Magnetoencephalography, Hertie-Institute for Clinical Brain Research, University of Tübingen, Tübingen, Germany
[2] Center for Integrative Neuroscience, University of Tübingen, Tübingen, Germany
[3] MEG-Center, University of Tübingen, Tübingen, Germany
[4] Institute for Modelling and Simulation of Biomechanical Systems, University of Stuttgart, Stuttgart, Germany
[5] Stuttgart Center for Simulation Science, University of Stuttgart, Stuttgart, Germany
* Author to whom any correspondence should be addressed.

**E-mail:** justus.marquetand@uni-tuebingen.de and justus.marquetand@imsb.uni-stuttgart.de

**Keywords:** muscle, OPM, quantum sensor, EMG, MMG, MFCV

Supplementary material for this article is available online

OPEN ACCESS

RECEIVED
18 December 2024

REVISED
21 March 2025

ACCEPTED FOR PUBLICATION
2 April 2025

PUBLISHED
16 April 2025



## Abstract

*Objective*. Muscle fiber conduction velocity (MFCV) describes the speed at which electrical activity propagates along muscle fibers and is typically assessed using invasive or surface electromyography. Because electrical currents generate magnetic fields, propagation velocity can potentially also be measured magnetically using magnetomyography (MMG), offering the advantage of a contactless approach. *Approach*. To test this hypothesis, we recorded MMG signals from the right biceps brachii muscle of 24 healthy subjects (12 male, 12 female) using a linear array of seven optically pumped magnetometers (OPMs). Subjects maintained muscle force for 30 s at 20%, 40%, and 60% of their maximum voluntary contraction. *Main results*. In 20 subjects, propagation of MMG signals was observable. Change in polarity and signal cancellation enabled localization of the innervation zone. We estimated the MFCV for each condition by cross-correlating double-differentiated MMG signals. To validate our results, we examined whether MFCV estimations increased with higher force levels, a well-documented characteristic of the neuromuscular system. The median MFCV significantly increased with force ($p = 0.007$), with median values of 3.2 m s $^{-1}$ at 20%, 3.8 m s $^{-1}$ at 40%, and 4.4 m s $^{-1}$ at 60% across all 20 subjects. *Significance*. Our results establish the first measurements of magnetic MFCV in MMG using OPMs. These findings pave the way for further developments and application of quantum sensors for contactless clinical neurophysiology.

## 1. Introduction

Muscle fiber conduction velocity (MFCV) is the speed of propagating electrical activity along muscle fibers. It is used in clinical diagnostics (Drost *et al* 2006, Campanini *et al* 2020) and research to detect neuromuscular disorders (Blijham *et al* 2011), assess muscle fatigue (Masuda *et al* 1999), or evaluate the effects of training or rehabilitation (Conrad *et al* 2017, Casolo *et al* 2020). The principle of measuring muscle fiber conduction velocity is based on the propagating electrical activity induced by motor neurons at their innervated muscle fibers (i.e. within the motor unit). These potentials propagate along the surface of the muscle fibers in both directions, starting from the so-called innervation zone (IZ) and moving toward the fiber ends (Heckman and Enoka 2004). This propagation is not stable over time; it varies according to age, sex, fatigue, training condition, or force (Farina and Merletti 2004b, Casolo *et al* 2020). Smaller motor units with lower conduction velocities are predominantly activated at lower force levels. As the force increases, larger motor units with fast-twitch fibers are progressively recruited, exhibiting higher conduction velocities due to their greater diameter (Del Vecchio *et al* 2018b, Casolo *et al* 2023). MFCV is

typically measured using electromyography (EMG), either invasively, by inserting needle electrodes directly into the muscle, or non-invasively, using surface electrodes placed on the skin. Multiple conduction velocities of many different motor units are included in global MFCV. If the MFCV of single motor units should be estimated, either decomposition methods of multiple signals or invasive EMG are necessary (Del Vecchio *et al* 2017). To calculate the conduction velocity in principle, the time difference (i.e. delay) between the same potential at two different locations is measured:

$$\mathrm{MFCV} = \frac{\text{Distance between electrodes}}{\text{Time difference between signals}}. \quad (1)$$

Acknowledging variations in signal shapes and experimental designs, various approaches have been developed to calculate the time difference between the signals during voluntary contractions or electrically evoked muscle responses. Reference points like local extrema, global extrema, or zero crossings can be used to estimate a delay (Farina and Merletti 2004a). Since these methods are sensitive to noise, the normalized cross-correlation is a common method to calculate the delay between similar signals:

$$\rho_{1,2}(\tau) = \frac{\sum_{n=1}^{N} x_2(n+\tau)\, x_1(n)}{\sqrt{\sum_{n=1}^{N} x_1^2(n) \sum_{n=1}^{N} x_2^2(n)}}. \quad (2)$$

The time point that maximizes the cross-correlation provides an estimate of the delay between signals with unequal shapes, where higher sampling rates or up-sampling will increase the resolution (Parker and Scott 1973, Farina and Merletti 2004b).

EMG and MFCV are well-established but have the inherent disadvantage of requiring contact through skin preparation (which is time-consuming and can cause skin irritation) or penetration (which can cause pain). This motivates the exploration of contactless alternatives. In recent years, there has been a notable advancement in the field of miniaturized magnetometers, which can measure the magnetic counterpart of electrical activity. This has led to the emergence of a novel modality, magnetomyography (MMG), a contactless and painless alternative to electromyography. MMG involves measuring magnetic fields generated by electrical currents, as described by the Biot–Savart law, which allows for assessing muscular activity without requiring direct contact with the skin or muscle. Although MMG was initially proposed in 1972 (Cohen and Givler 1972), its exploration has remained limited due to the technical constraints of bulky and spatially inflexible sensors, most importantly the superconducting quantum interference device (SQUID). SQUIDs are considered the gold standard for biomagnetic sensors but require cryogenic cooling to −268 °C. This necessitates a rigid design, limiting measurements to a predetermined shape and preventing adaptive or individualized sensor configurations, which are more suitable for MMG. Other more recent sensor technologies, such as tunnel magnetoresistance sensors and nitrogen-vacancy (NV) centers, though highly promising, have yet to demonstrate the capability to record MMG *in vivo* as they do not reach the necessary sensitivity beyond 1 pT/$\sqrt{\mathrm{Hz}}$. However, another class of magnetometers, optically pumped magnetometers (OPMs), are sensitive up to ∼15 fT $\sqrt{\mathrm{Hz}}$ and can be flexibly positioned to suit a subject's anatomy. This has led to a resurgence of interest in MMG (Kominis *et al* 2003, Boto *et al* 2017). Existing research indicates that MMG and EMG share similar signal characteristics, while MMG could offer advantages in comfort and speed (Broser *et al* 2021, Marquetand *et al* 2021, Ghahremani Arekhloo *et al* 2023). Additionally, MMG has the theoretical potential to detect signals from deeper muscle layers, thereby providing additional insights into neuromuscular physiology (Klotz *et al* 2023). In light of these considerations, an investigation into the potential of MMG for contactless recording and monitoring of neuromuscular changes, such as MFCV, represents a promising opportunity. It offers the prospect of a novel contactless muscle diagnostic for research and clinical applications, particularly in sports science.

## 2. Methods

### 2.1. Participants

Twenty-four healthy adults (12 females, 12 males) participated in this study, with a mean age of 28.6 ± 4.3 years and a mean body mass index of 22.2 ± 2.5 kg m$^{-2}$. Measurements were taken from the right biceps brachii muscle, a long and comparably low-pennated muscle. All participants reported no history of neuromuscular disorders. The study was approved by the research ethics committee of the University of Tübingen (797/2021BO2), and research was conducted in accordance with the principles embodied in the Declaration of Helsinki and in accordance with local regulatory requirements. Informed consent, including permission to participate and to publish data, was obtained from all participants. Considering previous EMG studies on MFCV often involved around 10 subjects (Farina and Merletti 2004a, Farina *et al* 2004b, Casolo *et al* 2020) and the fact that the signal-to-noise ratio (SNR) of MMG recordings might not be stable due to the movement-induced changes in the sensor to source distance, we increased this number to 24.

### 2.2. Experimental setup

MFCV estimation requires that sensors are aligned with the muscle fiber direction and that the sensors

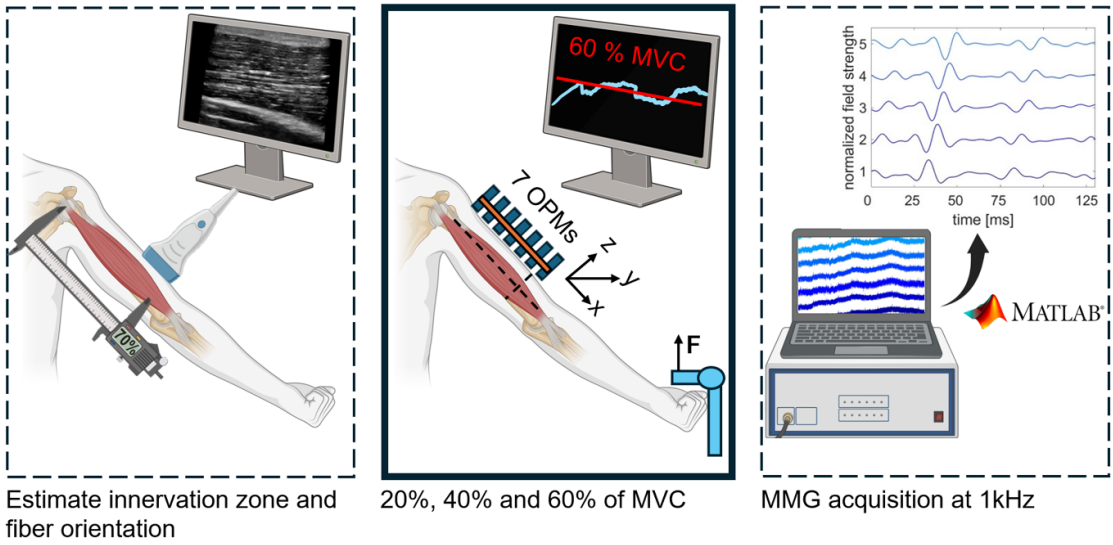


**Figure 1.** Illustration of the study protocol. (a) Anthropometric and ultrasonic measurements were conducted to estimate the location of the innervation zone and fiber orientation, respectively; (b) measurements were performed in a magnetically shielded room while the subjects executed steady contractions at 20%, 40%, and 60% of their maximum voluntary contraction (MVC). The *z*-axis of the OPM was pointing towards the muscle fiber as this configuration showed robust results in previous studies (Sometti *et al* 2021) (c) data acquisition for MMG was performed at a sampling rate of 1 kHz, and data processing was performed using MATLAB.

are located between the IZ and the myotendinous junction (Mito *et al* 2006, Nielsen *et al* 2008). Thus, the right biceps brachii muscle was selected due to its minimal muscle-skin distance, parallel fiber alignment, and extended fiber length on one side of the IZ (Saitou *et al* 2000, Barbero *et al* 2012). Ultrasonic imaging (Butterfly iQ+, Butterfly Network, Inc., Guilford, USA) was used to determine the muscle fiber orientation, which was marked on the skin. Further, the distance from the acromion to the elbow joint was measured, and 70% of this length was considered the IZ's location (Barbero *et al* 2012), as illustrated in figure 1(a). The study was conducted in a magnetically shielded room (Ak3b, VAC Vacuumschmelze, Hanau, Germany) at the MEG Center of the University of Tübingen, Germany. Participants removed all magnetic materials and changed into non-magnetic clothing to minimize interference. Participants were positioned supine in the shielded room, with the right forearm fixed in an anatomically adjusted setup to prevent biceps movement during measurement. Seven OPMs were placed close to the skin, aligned with the muscle fiber orientation. The distance from the center of the OPM's vapor cell to the skin was approximately 10 mm. The OPMs were positioned such that the first OPM is distal to the expected position of the IZ and the second OPM is proximal to the expected position of the IZ (figure 1(b)). Each participant performed a maximum voluntary contraction (MVC) to ensure no contact between the biceps muscle and the OPM sensors, thereby preventing artifacts caused by sensor movement in residual magnetic fields.

### 2.3. Force measurements

The apparatus fixed the elbow joint in a neutral-zero position and was equipped with a custom-built, non-magnetic force transducer connected to the participant's palm via an adjustable sling to prevent slack and ensure no pretension. The force transducer's analog output was amplified and processed using a data acquisition system (Quattrocento, OT Bioelectronica, Torino, Italy) managed by OT BioLab+ software. MVC measurements were conducted, and a relative scale was established for three target force levels. OT BioLab+ software provided live feedback from the force transducer, enabling the experimenter to monitor the force output at various levels. This data was provided audibly in real time to participants inside the shielded room to maintain steady force levels, as shown in figure 1.

### 2.4. Experimental protocol

From three MVC, the median force was used to establish each participant's individual MVC in OT BioLab +. At the beginning and end of the experiment, 30 s of baseline noise were recorded for MMG, with no participant involvement.

Participants were instructed to maintain 20%, 40%, and 60% of their MVC for 30 s each, with a 60-second rest period between efforts. Force levels were randomly ordered, i.e. increasing (20% to 40% to

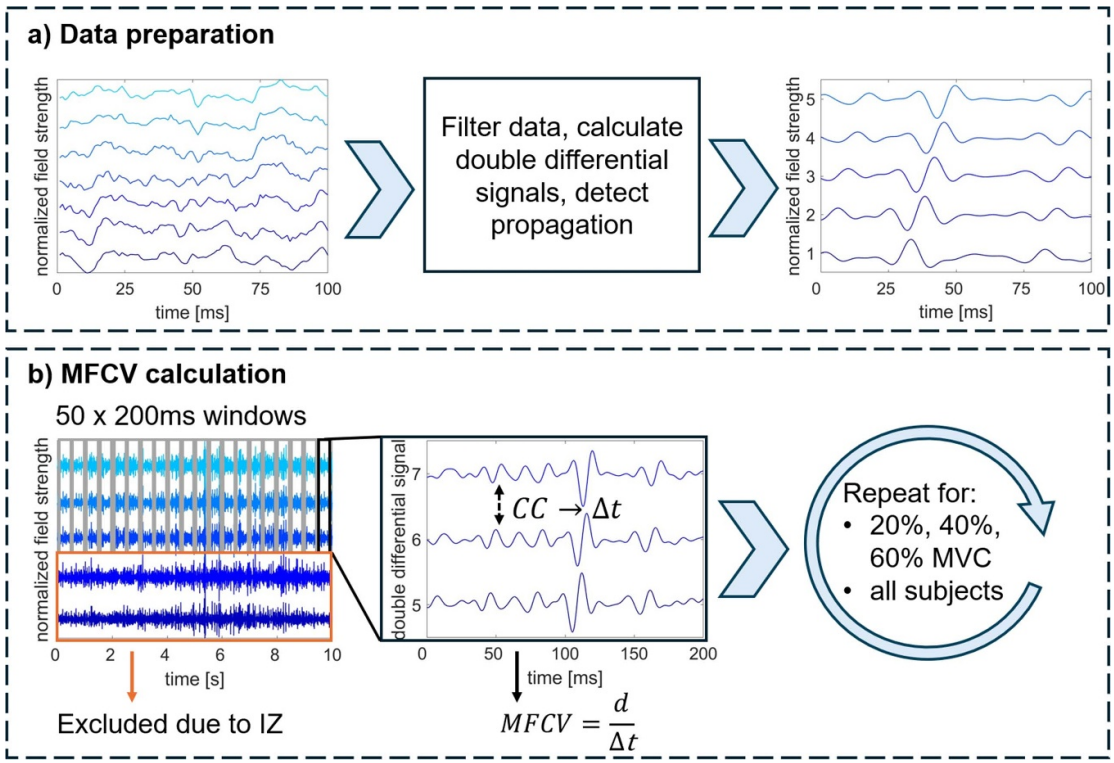


**Figure 2.** (a) Illustration of the data processing pipeline, including filtering, calculating double-differential signals, and visual inspection. (b) The middle ten seconds of the signals were divided into 50 windows. Cross-correlation is calculated for each window between the three most proximal signals (i.e. 3 top signals in the left panel furthest away from the innervation zone). This analysis was performed for 20%, 40%, and 60% of MVC for all subjects.

60%) or decreasing (60% to 40% to 20%). Given the constraints of the magnetically shielded room, participants received auditory feedback to help maintain the target force level throughout the task.

### 2.5. OPM-sensors, MMG-setup, and data acquisition

We used seven FieldLine Medical (v2, Boulder, Colorado, USA) OPMs. These rubidium-based OPMs have a bandwidth of 185 Hz, operate in a zero-field regime, and their sensing vapor cell is 5 mm distant from the outer surface of the sensor housing. All OPMs were operated in closed-loop mode and were recalibrated before measuring each new force level. OPMs were arranged in a linear configuration within a custom-made, 3D-printed housing to measure the change in magnetic fields and, consequently, the propagation along a muscle fiber. Each OPM measured 13 mm by 15 mm by 30 mm. The distance between the vapor cells of successive OPMs was 18 mm. Data acquisition was performed at 1000 Hz using the FieldLine Medical acquisition device.

### 2.6. Data analysis and processing

All data analyses were performed in Matlab (MathWorks, R2023b) using custom scripts and the open-source toolbox Fieldtrip (Oostenveld *et al* 2011). After visual inspection, MMG data were digitally bandpass filtered using a zero phase first-order Butterworth filter between 25 and 100 Hz. Preliminary studies indicated that the highest signal agreement with the EMG was observed in this frequency range. Line noise was attenuated using a zero phase first order band-stop Butterworth filter (49-51 Hz). The data were upsampled and interpolated to a sampling rate of 10 kHz. Double differential derivations ($DD_i(t)$) along the muscle fiber were computed, with $S_i$ representing the signal observed at the *i*th sensor:

$$DD_i(t) = -S_{i+1}(t) + 2 \cdot S_i(t) - S_{i-1}(t). \quad (3)$$

An experienced investigator visually inspected all magnetic field component signals and double differential signals to determine whether the signals showed propagating components and a directional change of the propagation (i.e. an indicator of an IZ), see figures 2 and 3. For each force level, the middle 10 s was segmented into 50 windows, each with a duration of 200 ms (Del Vecchio *et al* 2018a). Due to the potential impact of the IZ, sensors 1 and 2 (i.e. the two most distal sensors) were excluded for further MFCV calculation. The double DD from sensors 3–7 yielded three double-differential signals. Cross-correlation was calculated for each window and was used to estimate the MFCV between the double DD.

Corresponding with previous EMG studies, only physiological values within the range of 2 m $s^{1}$–8 m $s^{-1}$ were accepted (Beretta-Piccoli *et al* 2019). Global MFCVs were determined by calculating the median MFCVs of all 50 windows for each force level and subject separately. Furthermore, for each subject, we calculated the averaged root mean square (RMS) values for noise recordings and each different force level using the 10 s mid-recording window of each condition.

### 2.7. Statistics

All sociodemographic, morphometric, and pre-processed MMG data were statistically analyzed using MATLAB. In addition to descriptive statistics, the normality of distributions was assessed using the Shapiro-Wilk test. Since the data were not normally distributed, the Friedman test was employed, followed by the post-hoc Dunn-Bonferroni method for pairwise comparisons. The coefficient of variation was estimated by the mean absolute deviation divided by the median, multiplied by 1.48.

## 3. Results

In 20 out of 24 subjects, visual inspection showed neuromuscular propagation for all force levels. Four subjects were excluded due to no visible propagation (3 females, 1 male, mean age of 27 $\pm$ 5.3 years, mean body mass index of 22.1 $\pm$ 2.6 kg $m^{-2}$). Consequently, 20 subjects were used for further analysis.

### 3.1. Innervation zone

The location of the IZ was estimated whenever a change in the conduction direction was visible and was possible for 18 subjects. Two subjects revealed a continuous propagation direction, thus indicating that the IZ was located distal to the sensor placement. Those 20 subjects were used for further MFCV estimation. Figure 3 exemplarily illustrates that an IZ is further characterized by a change in the magnetic field's polarity (in all subjects) as well as magnetic field cancellation (observed in 6 out of 20 subjects).

### 3.2. Relationship between MFCV and force

For most subjects (17 out of 20), MFCV monotonically increased with force. Only 3 subjects (subjects 5, 15, and 16) showed non-monotonic behavior (see figure 4). At the group level, the median values were 3.1 m $s^{-1}$ for 20% MVC, 3.6 m $s^{-1}$ for 40% MVC, and 4.4 m $s^{-1}$ for 60% individual MVC. Friedman's test revealed a statistically significant effect of force level on MFCV (Chi2 = 37.03; $p < 0.001$). Post-hoc pairwise comparisons using the Dunn-Bonferroni method revealed significantly different MFCV values between all force levels (20% vs. 40%: $p = 0.007$; 20% vs. 60%: $p < 0.001$; 40% vs. 60%: $p = 0.007$). The estimated coefficient of variation of MFCV on the group level was 15.0% at 20% MVC, 12.3% at 40% MVC, and 14.2% at 60% MVC. Moreover, the greater the force, the larger the average RMS of MMG across all OPMs ($p < 0.001$, post-hoc pairwise comparison, figure 5. For information on individual OPMs, see supplemental figure 1).

### 3.3. Amplitude and noise characterization

The RMS was calculated to quantify the amplitude of the measured magnetic fields, using the middle ten seconds for each subject and force level. Figure 5 summarizes the mean and standard deviation of the RMS values, averaged across all sensors. Further, the RMS at each OPM sensor is given in supplementary figure 1. The RMS of noise levels was found to be within the range of 0.25 $\pm$ 0.05 pT for all subjects. In contrast, the RMS of force levels exhibited an increase from 1.01 $\pm$ 0.18 pT at 20% MVC to 1.97 $\pm$ 0.37 pT at 40% MVC and 3.41 $\pm$ 0.71 pT at 60% MVC. SNR was calculated for each subject based on RMS values, as shown in figure 5. The SNR increased with contraction intensity, from 11.10 $\pm$ 4.13 dB to 16.67 $\pm$ 4.70 dB to 21.37 $\pm$ 5.24 dB.

## 4. Discussion

Here, we demonstrated in 20 healthy adults that it is possible to measure the MFCV and localize the IZ of a human muscle without contact. The correlation between force and MFCV falls within the range reported in the literature using different EMG methods for the biceps brachii muscle (Li and Sakamoto 1996, Rainoldi *et al* 1999, Beretta-Piccoli *et al* 2018) and can serve as a valuable reference for future MMG studies on MFCV.

A contactless measurement of MFCV is promising for clinical application. Although the measurement of electrical MFCV using surface EMG is well-established, it has not made its way into the daily clinical routine due to the time-intensive nature of skin preparation and electrode placement, as well as the robustness of the method. In contrast, magnetic MFCV measurement using OPM-MMG eliminates the need for skin and electrode preparation, as it only requires positioning the muscle next to an array of sensors in a shielded room. This underscores its potential as a contactless, painless diagnostic and monitoring tool for clinical practice and applied physiology (e.g. sports science). This contactless approach may not only broaden the use of MFCV in clinical routines but also facilitate the translation of metrics from sports science into everyday medical practice. Our results support the hypothesis that magnetically, MFCV shares the same characteristics as reported by EMG and promotes both MFCV and OPM-MMG for clinical use.

Detecting the IZ is essential for accurately estimating MFCV, as placing electrodes or sensors (here

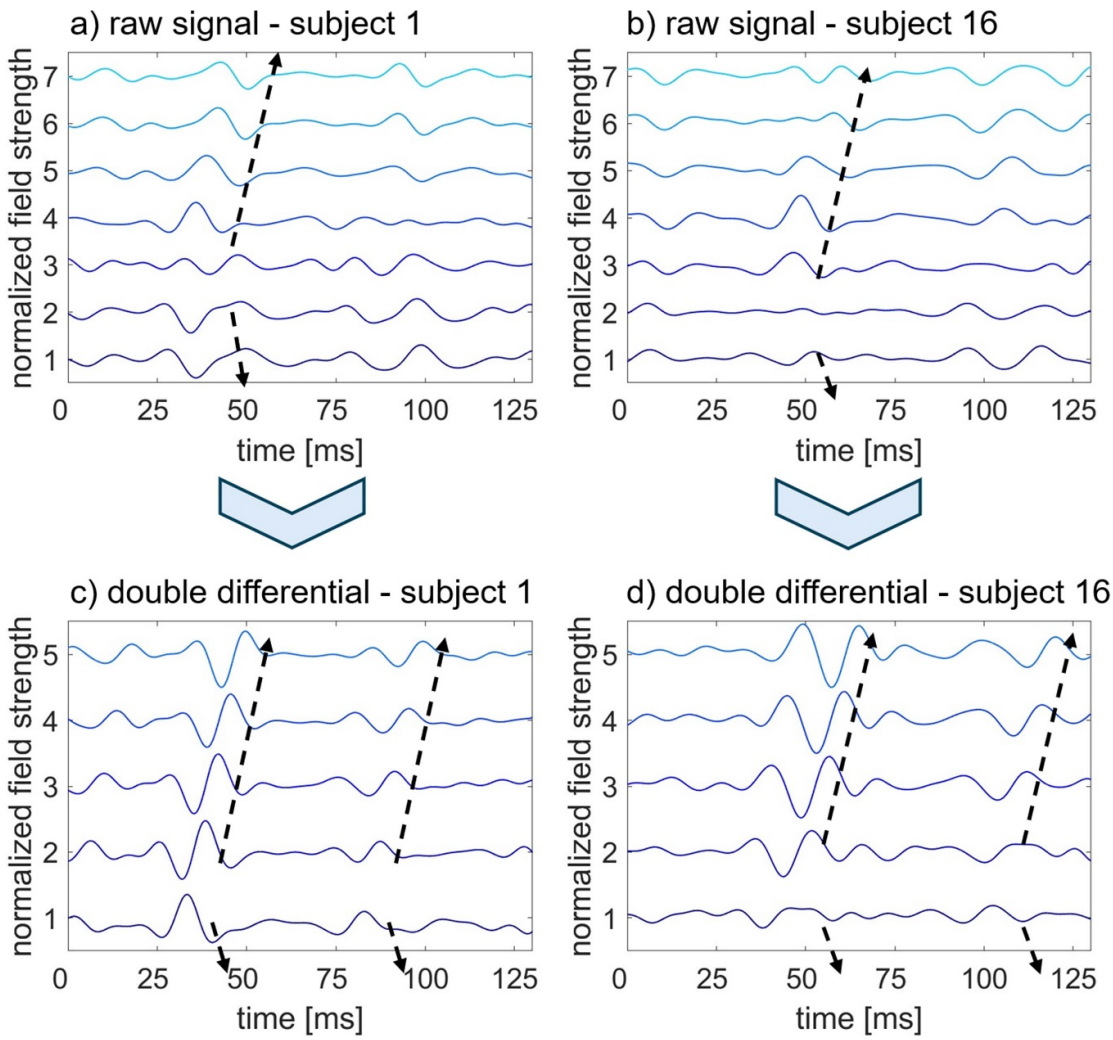


**Figure 3.** Pre-processed data shows the propagation of potentials (subjects 1 and 16 in panels a and b, respectively) during voluntary contraction. Double differential derivations from seven OPM channels produce five signals of the same subjects (subjects 1 and 16 in panels c and d, respectively). The top signal is the most proximal, and signal 1 is the most distal. Arrows indicate visible propagation of motor unit action potentials. (a) Propagation in both directions and magnetic field's polarity change estimates the innervation zone between signals 2 and 3. (b) Propagation, magnetic field's polarity change and magnetic field cancellation of signal 2 estimates the innervation zone close to signal 2. (c) and (d): Double differential signals increase the visibility of propagating action potentials and are necessary for further delay estimation.

OPM) directly over the IZ can cause artifacts, leading to unreliable MFCV measurements. Thus, proper localization of the IZ ensures optimal sensor placement along the muscle fiber direction and is essential for robust MFCV estimation.

Our study demonstrates that OPM-MMG arrays directly enable the detection of the IZ. In detail, at the sensor level, the IZ is characterized by changes in magnetic field polarity or magnetic field cancellation (see figure 3). Although we did not precisely register each OPM to the respective individual anatomy, the IZ consistently was found to be approximately in the expected distal third of the biceps brachii muscle.

Previous studies showed electrically (EMG) measured MFCV effects according to force (Zwarts and Arendt-Nielsen 1988, Farina *et al* 2004a, Casolo *et al* 2020). Force-correlated recruitment of motor units containing fibers with greater diameters is decisive. We observed a similar behavior for MMG. We showed that magnetically (MMG) measured MFCV increases significantly with each increase in force level on an individual level (figure 4). However, three subjects did not increase the MFCV across all force levels. The reason could be the movement of the subject's biceps muscle in between force levels, leading to a lower signal amplitude due to an increased sensor-to-source distance. Moreover, any lateral movement would lead to a measurement of a different subset of muscle fibers. Fiber diameter, inhomogeneities, or local metabolic conditions would lead to another global propagation speed. Optical distance and localization control (e.g. localization coils) could be used in further studies to prevent this.

We excluded four subjects from the analysis as we could not reliably observe neuromuscular propagation by visual inspection. These could be due to several reasons: (1) Participant movement during the experiment, particularly during contraction, may

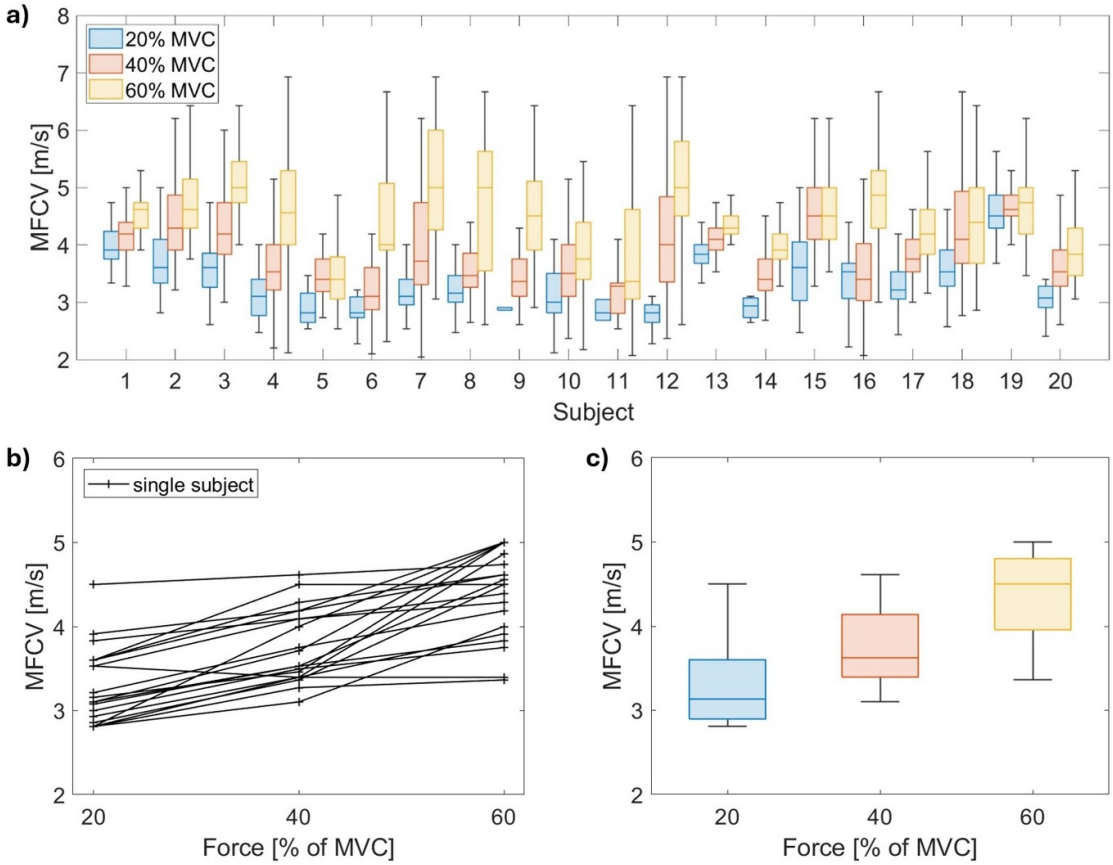


**Figure 4.** (a) Individual muscle fiber conduction velocity (MFCV) across subjects for 20%, 40%, and 60% MVC. MFCV was calculated using cross-correlation for 20 windows with a length of 500 ms (see also figure 1). (b) Individual median MFCV across the applied force, which illustrates an individual increase of MFCV with increasing force levels. (c) A group-level comparison of all 20 subjects will be conducted, providing a perspective on the relationship between MFCV and applied force levels as described.

| | RMS | | | | | | | | SNR | | |
|---|---|---|---|---|---|---|---|---|---|---|---|
| | Noise | | 20% MVC | | 40% MVC | | 60% MVC | | | | |
| Subject | Mean | SD | Mean | SD | Mean | SD | Mean | SD | 20% MVC | 40% MVC | 60% MVC |
| 1 | 0.28 | 0.03 | 0.74 | 0.26 | 1.04 | 0.37 | 2.02 | 1.02 | 8.41 | 11.36 | 17.08 |
| 2 | 0.25 | 0.03 | 1.00 | 0.18 | 2.41 | 0.53 | 3.18 | 0.72 | 12.16 | 19.79 | 22.22 |
| 3 | 0.26 | 0.05 | 1.04 | 0.09 | 1.79 | 0.32 | 2.89 | 0.52 | 11.97 | 16.72 | 20.87 |
| 4 | 0.23 | 0.05 | 0.67 | 0.10 | 1.29 | 0.24 | 2.99 | 0.61 | 9.23 | 14.89 | 22.21 |
| 5 | 0.24 | 0.04 | 1.38 | 0.12 | 1.97 | 0.15 | 1.86 | 0.27 | 15.03 | 18.10 | 17.64 |
| 6 | 0.23 | 0.04 | 0.70 | 0.09 | 1.80 | 0.28 | 5.98 | 1.29 | 9.85 | 18.02 | 28.44 |
| 7 | 0.35 | 0.04 | 1.34 | 0.13 | 2.06 | 0.26 | 4.18 | 0.72 | 11.66 | 15.36 | 21.52 |
| 8 | 0.23 | 0.06 | 1.13 | 0.17 | 2.03 | 0.35 | 5.01 | 1.27 | 13.80 | 18.87 | 26.72 |
| 9 | 0.24 | 0.05 | 0.81 | 0.14 | 1.20 | 0.27 | 1.81 | 0.39 | 10.43 | 13.82 | 17.37 |
| 10 | 0.23 | 0.06 | 0.77 | 0.13 | 1.72 | 0.34 | 2.32 | 0.47 | 10.39 | 17.43 | 20.02 |
| 11 | 0.25 | 0.04 | 0.44 | 0.03 | 0.86 | 0.07 | 1.47 | 0.14 | 4.85 | 10.72 | 15.44 |
| 12 | 0.26 | 0.04 | 1.11 | 0.28 | 2.22 | 0.32 | 4.42 | 0.64 | 12.49 | 18.52 | 24.50 |
| 13 | 0.24 | 0.05 | 1.61 | 0.32 | 3.97 | 0.93 | 6.61 | 1.20 | 16.39 | 24.23 | 28.65 |
| 14 | 0.24 | 0.06 | 0.49 | 0.12 | 0.96 | 0.09 | 1.52 | 0.33 | 6.17 | 12.02 | 15.96 |
| 15 | 0.23 | 0.06 | 0.66 | 0.08 | 2.16 | 0.39 | 3.65 | 0.85 | 9.15 | 19.46 | 24.03 |
| 16 | 0.24 | 0.04 | 2.14 | 0.35 | 4.93 | 0.83 | 5.68 | 1.32 | 19.11 | 26.36 | 27.59 |
| 17 | 0.28 | 0.04 | 0.88 | 0.18 | 1.68 | 0.29 | 3.90 | 0.68 | 9.91 | 15.49 | 22.80 |
| 18 | 0.26 | 0.06 | 0.87 | 0.30 | 1.60 | 0.61 | 2.54 | 0.83 | 10.58 | 15.93 | 19.94 |
| 19 | 0.32 | 0.05 | 1.76 | 0.31 | 4.39 | 0.87 | 5.72 | 0.74 | 14.85 | 22.81 | 25.10 |
| 20 | 0.25 | 0.06 | 0.51 | 0.09 | 1.07 | 0.23 | 2.03 | 0.40 | 6.16 | 12.54 | 18.15 |



**Figure 5.** Root mean square values (RMS) and signal-to-noise ratio (SNR) from 20 subjects across three force levels (20%, 40%, 60% MVC) averaged over seven sensors. Left: Noise RMS, mean and standard deviation of RMS in Picotesla ($10^{-12}$ Tesla). Right: SNR in dB. A color scale illustrates RMS and SNR increase as force levels rise.

have shifted the biceps muscle beyond the optimal detection range of the OPMs, reducing spatial resolution and the ability to resolve distinct neuromuscular activities. This is analogous to enlarging the recording area of EMG electrodes. (2) Participant movements during the recording may have altered not only the distance but also the geometry between the muscle fibers and the OPM sensors, potentially impairing the accurate measurement of magnetic muscle activity. Misalignment of the used uniaxial OPMs, oriented in the $z$-direction according to the muscle fibers (figure 1), could limit the detection of signal propagation, similar to alignment challenges seen in EMG when studying muscle fiber conduction velocity. While the spatial sensitivity of MMG poses challenges, it also offers advantages, as triaxial OPM arrays could significantly improve the resolution of distinct neuromuscular signals. This promising avenue lies beyond the current study and warrants further experimental investigation. (3) Despite careful visual inspection of each participant's recording, the potential influence of environmental magnetic artifacts on signal quality cannot be entirely ruled out. In addition, touching the sensors during the experiment can cause the OPMs to oscillate in residual magnetic fields, affecting signal quality. (4) A thicker subcutaneous fat layer, which was not measured in all participants, may have diminished signal quality. The higher dropout rate among female participants supports this hypothesis, as women typically have thicker subcutaneous fat layers than men, particularly in the upper body region (Hattori *et al* 1991).

Further studies are required to investigate these potential factors and to further improve the robustness of OPM-MMG for measuring MFCV.

The further application of the magnetic MFCV provides insights into neuromuscular health, offering applications in diagnosis, monitoring, and therapeutic evaluation. In clinical diagnostics, MFCV aids in distinguishing or identifying different neuromuscular disorders. Particularly in pediatrics, MFCV might be important for early detection of neuromuscular changes, as children may exhibit greater tolerance for contactless measurement methods compared to those requiring physical contact (Boto *et al* 2022). MFCV also detects metabolic changes like muscle fatigue during sustained contractions. In rehabilitation, MFCV enables recovery tracking and assesses adaptations to therapy or training. Furthermore, MFCV reflects muscle fiber composition, providing information relevant to age-related muscle decline, athletic performance, and systemic diseases such as diabetic neuropathy and chronic conditions. The current potential of MMG is comparable to the advancements brought by HD-sEMG in studying neuromuscular activity. However, despite its capabilities, HD-sEMG has seen limited adoption in clinical settings due to challenges such as time-intensive preparation, complex post-processing, and a preference for invasive EMG, which remains the gold standard due to its cost-effectiveness, speed, reliability, and ability to detect highly localized signals. MMG could bridge this gap, as it eliminates preparation time while offering signal content comparable to HD-sEMG. MMG's practical potential is particularly evident in three scenarios: (1) patient populations intolerant to invasive EMG or skin preparation, such as infants, children, individuals with dementia, or burn victims; (2) cases requiring a holistic view of neuromuscular activity, such as in neuromuscular disorders where altered activation patterns (Semeia *et al* 2022) and motor unit recruitment serve as biomarkers of disease (e.g. motor neuron diseases such as amyotrophic lateral sclerosis or neuromuscular junction disorders such as myasthenia gravis), with motor unit decomposition using OPM arrays (Noury *et al* 2024); and (3) repetitive monitoring in rehabilitation medicine, such as for stroke survivors or patients with progressive neuromuscular disorders, where MMG's contactless nature avoids skin irritation. These applications highlight MMG's value in pain-sensitive populations and scenarios requiring comprehensive neuromuscular assessment. These insights could guide interventions, optimize treatments, and monitor progression.

Our findings demonstrate that MMG RMS increases with force level. While a detailed analysis of individual sensor distributions was beyond the scope of this study, the additional data provided will facilitate future investigations into MMG signal variability and SNR optimization. A key challenge in MMG studies is the strong dependency of SNR on sensor-to-source distance. Although an ideal setup would maintain a constant sensor-to-source distance, the dynamic curvature of the biceps during contraction leads to unavoidable variations when using a planar linear array, as in our study. While this remains an active area of research, we consider this effect negligible for MFCV estimation in our proof-of-feasibility design. To ensure transparency, we have also reported both the average signal RMS and SNR at different force levels as well as noise RMS per subject, allowing for direct comparison with future studies (figure 5).

### 4.1. Strengths and limitations

The primary limitation of the experiments is the absence of a ground truth within each subject. Given the considerable temporal and spatial variability inherent to global MFCV, it is only possible to make exact comparisons at the local level, specifically between the same single motor units in EMG and MMG.

Nevertheless, this necessitates the implementation of a simultaneous recording utilizing a high-density surface EMG. Subsequently, a motor unit decomposition in both EMG and MMG could be employed to identify the associated motor units, facilitating an optimal comparison. Indeed, motor unit decomposition in MMG has recently been established

(Noury *et al* 2024). Moreover, factors such as muscle size, training habits, fiber type, age or sex have yet to be systematically explored, as they have been in EMG research (Cruz Martínez and López Terradas 1990, Kupa *et al* 1995). In particular, the influence of varying pennation angles across different muscle types on magnetic MFCV remains an important spatial challenge. While current miniaturized OPMs are available, their size—larger than conventional surface electrodes—makes measuring small muscles challenging, if not impractical.

Using cross-correlation for sEMG, a higher correlation coefficient is expected to ensure the reliability of signal-matching (Beretta-Piccoli *et al* 2019, Casolo *et al* 2020). As we use different sensors with no common ground, the signal shapes vary greatly depending on the spatial position. Therefore, using the same correlation coefficient from EMG will not work in MMG. In sEMG, a maximum likelihood estimator can reduce the standard deviation by minimizing the mean square error (Farina *et al* 2004b). However, this method did not lead to reasonable results in MMG for the same reasons mentioned above. Therefore, cross-correlation was used due to its traceability and transparency. Although our work highlights the potential of MMG in general and OPM-MMG in particular, its translation into daily clinical practice remains unestablished, necessitating further studies to assess the reliability and validity of MMG across diverse measurement scenarios. Although OPMs are less expensive than SQUIDs, the cost of acquiring two or three OPMs, along with the required magnetic shielding, is currently similar to that of a standard EMG amplifier with preamplifiers and electrodes. Additionally, practical advancements toward portability and a comprehensive turnkey solution for clinical use have yet to be realized. With growing interest in OPMs within the scientific community, sensor costs—and potentially magnetic shielding costs—are expected to decrease. Nevertheless, significant technological development is required for their integration into routine clinical applications.

### 4.2. Conclusion

Conduction velocity within a muscle fiber can be calculated by measuring magnetic fields using OPM. In general, neuromuscular activity and IZ propagation are visible in MMG. MMG can measure MFCV using magnetic fields arising from neuromuscular activity, exhibiting the same characteristics as EMG. Comparing properties of single motor units in MMG and EMG is essential for further understanding and comparison of both modalities.

## Data availability statement

The data that support the findings of this study are available upon reasonable request from the authors.

## Acknowledgment

The authors thank all the participants for their time, effort, and commitment to this study. Their contributions were invaluable, and this research would not have been possible without their dedication and support.

L B is supported by the Johannes-Dichgans-scholarship of the Hertie-Institute for Clinical Brain Research. B S, T K, J M are supported by the Deutsche Forschungsgemeinschaft (DFG, German ResearchFoundation) through the priority program SPP 2311 (Grant ID. 548605919). A K, T K, J M, O R are supported by the European Research Council (ERC) through the ERC-AdG 'qMOTION' (Grant ID. 101055186). J M, N N are supported by the Bundesministerium für Bildung und Forschung (BMBF) through the Future-Cluster 'QSens' (Grant ID. 03ZU2110FD).

## ORCID iDs

Lukas Baier https://orcid.org/0009-0008-6367-8851
Burak Senay https://orcid.org/0009-0009-7654-5844
Thomas Klotz https://orcid.org/0000-0002-0503-9815
Justus Marquetand https://orcid.org/0000-0002-2039-5498

## References

Barbero M, Merletti R and Rainoldi A 2012 *Atlas of Muscle Innervation Zones: Understanding Surface Electromyography and Its Applications* (Springer) (https://doi.org/10.1007/978-88-470-2463-2)

Beretta-Piccoli M *et al* 2018 Relationship between isometric muscle force and fractal dimension of surface electromyogram *Biomed. Res. Int.* **2018** 5373846

Beretta-Piccoli M *et al* 2019 Reliability of surface electromyography in estimating muscle fiber conduction velocity: a systematic review *J. Electromyogr. Kinesiol.* **48** 53–68

Blijham P J *et al* 2011 Diagnostic yield of muscle fibre conduction velocity in myopathies *J. Neurol. Sci.* **309** 40–44

Boto E *et al* 2017 A new generation of magnetoencephalography: room temperature measurements using optically-pumped magnetometers *NeuroImage* **149** 404–14

Boto E *et al* 2022 Triaxial detection of the neuromagnetic field using optically-pumped magnetometry: feasibility and application in children *NeuroImage* **252** 119027

Broser P J *et al* 2021 Optically pumped magnetometers disclose magnetic field components of the muscular action potential *J. Electromyogr. Kinesiol.* **56** 102490

Campanini I *et al* 2020 Surface EMG in clinical assessment and neurorehabilitation: barriers limiting its use *Front. Neurol.* **11** 934

Casolo A *et al* 2023 Non-invasive estimation of muscle fibre size from high-density electromyography *J. Physiol.* **601** 1831–50

Casolo A, Farina D, Falla D, Bazzucchi I, Felici F and Del Vecchio A 2020 Strength training increases conduction velocity of high-threshold motor units *Med. Sci. Sports Exercise* **52** 955

Casolo A, Nuccio S, Bazzucchi I, Felici F and Del Vecchio A 2020 Reproducibility of muscle fibre conduction velocity during linearly increasing force contractions *J. Electromyogr. Kinesiol.* **53** 102439

Cohen D and Givler E 1972 Magnetomyography: magnetic fields around the human body produced by skeletal muscles *Appl. Phys. Lett.* **21** 114–6

Conrad M O *et al* 2017 Analysis of muscle fiber conduction velocity during finger flexion and extension after stroke *Topic Stroke Rehabil.* **24** 262–8

Cruz Martínez A and López Terradas J M 1990 Conduction velocity along muscle fibers *in situ* in healthy infants *Electromyogr. Clin. Neurophysiol.* **30** 443–8

Del Vecchio A *et al* 2017 Associations between motor unit action potential parameters and surface EMG features *J. Appl. Physiol.* **123** 835–43

Del Vecchio A, Bazzucchi I and Felici F 2018a Variability of estimates of muscle fiber conduction velocity and surface EMG amplitude across subjects and processing intervals *J. Electromyogr. Kinesiol.* **40** 102–9

Del Vecchio A, Negro F, Felici F and Farina D 2018b Distribution of muscle fibre conduction velocity for representative samples of motor units in the full recruitment range of the tibialis anterior muscle *Acta Physiol.* **222** e12930

Drost G *et al* 2006 Clinical applications of high-density surface EMG: a systematic review *J. Electromyogr. Kinesiol.* **16** 586–602

Farina D, Macaluso A, Ferguson R A and De Vito G 2004a Effect of power, pedal rate, and force on average muscle fiber conduction velocity during cycling *J. Appl. Physiol.* **97** 2035–41

Farina D and Merletti R 2004a Methods for estimating muscle fibre conduction velocity from surface electromyographic signals *Med. Biol. Eng. Comput.* **42** 432–45

Farina D and Merletti R 2004b Estimation of average muscle fiber conduction velocity from two-dimensional surface EMG recordings *J. Neurosci. Methods* **134** 199–208

Farina D, Pozzo M, Merlo E, Bottin A and Merletti R 2004b Assessment of average muscle fiber conduction velocity from surface EMG signals during fatiguing dynamic contractions *IEEE Trans. Biomed. Eng.* **51** 1383–93

Ghahremani Arekhloo N *et al* 2023 Alignment of magnetic sensing and clinical magnetomyography *Front. Neurosci.* **17** 1154572

Hattori K *et al* 1991 Sex differences in the distribution of subcutaneous and internal fat *Hum. Biol.* **63** 53–63

Heckman C J and Enoka R 2004 Physiology of the motor neuron and the motor unit *Handbook of Clinical Neurophysiology* vol 4, ed A Eisen (Elsevier) pp 119–47

Klotz T *et al* 2023 High-density magnetomyography is superior to high-density surface electromyography for motor unit decomposition: a simulation study *J. Neural Eng.* **20** 046022

Kominis I K *et al* 2003 A subfemtotesla multichannel atomic magnetometer *Nature* **422** 596–9

Kupa E J *et al* 1995 Effects of muscle fiber type and size on EMG median frequency and conduction velocity *J. Appl. Physiol.* **79** 23–32

Li W and Sakamoto K 1996 Distribution of muscle fiber conduction velocity of M. biceps brachii during voluntary isometric contraction with use of surface array electrodes *Appl. Hum. Sci.* **15** 41–53

Marquetand J *et al* 2021 Optically pumped magnetometers reveal fasciculations non-invasively *Clin. Neurophysiol.* **132** 2681–4

Masuda K *et al* 1999 Changes in surface EMG parameters during static and dynamic fatiguing contractions *J. Electromyogr. Kinesiol.* **9** 39–46

Mito K *et al* 2006 Comparison of experimental and numerical muscle fiber conduction velocity (MFCV) distribution around the end-plate zone and fiber endings *Med. Sci. Monit.* **12** BR115–23

Nielsen M, Graven-Nielsen T and Farina D 2008 Effect of innervation-zone distribution on estimates of average muscle-fiber conduction velocity *Muscle Nerve* **37** 68–78

Noury N *et al* 2024 Detecting single motor-unit activity in magnetomyography *bioRxiv* p 2024

Oostenveld R *et al* 2011 FieldTrip: open source software for advanced analysis of MEG, EEG, and invasive electrophysiological data *Comput. Intell. Neurosci.* **2011** 1–9

Parker P A and Scott R N 1973 Statistics of the myoelectric signal from monopolar and bipolar electrodes *Med. Biol. Eng.* **11** 591–6

Rainoldi A, Galardi G, Maderna L, Comi G, Lo Conte L and Merletti R 1999 Repeatability of surface EMG variables during voluntary isometric contractions of the biceps brachii muscle *J. Electromyogr. Kinesiol.* **9** 105–19

Saitou K, Masuda T, Michikami D, Kojima R, Okada M 2000 Innervation zones of the upper and lower limb muscles estimated by using multichannel surface EMG *J. Hum. Ergol.* **29** 35–52

Semeia L *et al* 2022 Optically pumped magnetometers detect altered maximal muscle activity in neuromuscular disease *Front. Neurosci.* **16** 1010242

Sometti D *et al* 2021 Muscle fatigue revisited—insights from optically pumped magnetometers *Front. Physiol.* **12** 724755

Zwarts M J and Arendt-Nielsen L 1988 The influence of force and circulation on average muscle fibre conduction velocity during local muscle fatigue *Eur. J. Appl. Physiol. Occup. Physiol.* **58** 278–83